Residual Gas, Emittance Growth and Beam Lifetime in Tevatron at 150 GeV

V. A. Lebedev, L. Y. Nicolas[†], A. V. Tollestrup
Fermi National Accelerator Laboratory
P.O. Box 500, Batavia, Illinois 60510, USA
[†] *Also Department of Physics & Astronomy*
University Of Glasgow, Glasgow, UK

February 26, 2004

Abstract

The note presents the studies conducted in June 2003 with the Tevatron proton beam at 150 GeV to investigate vacuum conditions and beam lifetime.

1 Introduction

Beam interactions with the residual gas inside the Tevatron beam pipe are partly responsible for the emittance growth (elastic scattering) and loss of particles (inelastic scattering), thus degradation of the luminosity [1]. It is therefore important to determine the current gas composition and pressure in the Tevatron, and devices such as residual gas analyzer (RGA) are used for that purpose. However, the number of RGA's placed along the $2\pi \times 1000$ meters of the ring is limited, providing a local information only, and although they have a good atomic mass resolution, the partial pressure they give for each gas can be an order of magnitude higher than what it actually is [2]. It is possible to obtain an average global picture of these values by analyzing the beam characteristics such as lifetime and diffusion factor, using an elaborated model for the beam emittance growth [3], and experimental data from dedicated Tevatron studies.

2 Experimental Protocol

Several different processes are responsible for the beam halo formation [4]. Since this study aims at the residual gas investigation, the experimental conditions had to be such that every other mechanisms were minimized and leave beam-gas interactions as the dominant effect. An uncoalesced beam of 150 GeV protons was thus injected in the machine on a central orbit with a total intensity of about 6×10^{11} protons, to mitigate intra-beam scattering. To prevent particles from leaking out of the bucket due to RF noise, the beam was then debunched by removing the RF.
The experiment is based on partial scraping of the beam, leaving a zone of high diffusion when the beam is left by itself interacting with gas. The halo population immediately outside the beam core is dominated by the diffusion caused by multiple Coulomb scattering, whereas further away, it is more driven by single nuclear scattering and single Coulomb scattering. The transverse halo growth is not the same for vertical and horizontal planes, the horizontal one involving more different halo generation mechanisms than the vertical one [5], therefore the collimator used for the beam scraping was the D49V vertical jaw where the dispersion $\frac{\Delta p}{p}$ is minimal. A preliminary scraping with a horizontal collimator was also done in order to prepare the beam for the experiment, and it is assumed that coupling between both transverse planes is negligible, so that a unidimensional treatment is considered in this note.
The systematics of the experiment performed with the help of D. Still were as follows:

1. 1st measurement: The beam was injected and partially scraped horizontally, then totally scraped with D49V, constituting the first reference.

2. 2nd measurement: Another injection followed with the same conditions, but the vertical scraping stopped before the removal of the beam around an intensity of 2×10^{11} protons, and the beam stayed by itself for 1.5 hours, before being fully scraped.

3. 3rd measurement: A third injection and scraping constitute the second reference.

During all the measurements, the beam intensity, collimator positions and the signal from one beam loss monitor were recorded. Fig. 1(left) shows the evolution of the beam current in the Tevatron from the ACNET variable IBEAM, Fig. 1(right) displays IBEAMS (IBEAM Small) which saturates around 2×10^{11} p and was preferably used for the analysis due to its better resolution.

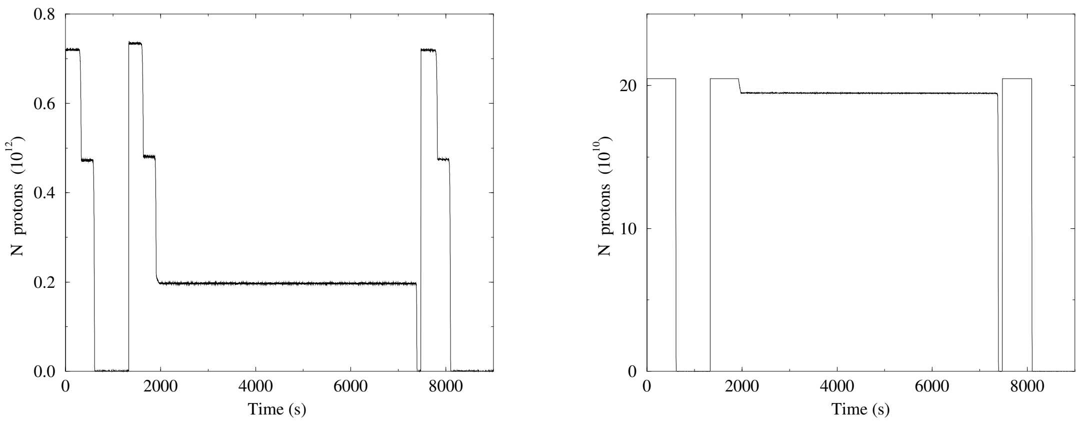

Figure 1: Evolution of the Tevatron beam intensity: IBEAM (left) and IBEAMS (right).

3 Analysis

The analysis has three parts, the beam size and emittance, the diffusion coefficient and emittance growth, and the beam lifetime with vacuum study.

3.1 Beam size

The determination of the beam size (and thus emittance) is done by investigating the shape of IBEAM when the current vanishes during vertical scraping. An example is given in Fig. 2 (left). The x-axis corresponds to the vertical collimator position that is pushed toward the beam from the outside of the beam pipe up to the extinction of the current (around -28 mm). In this plot the collimator goes from right to left, and only starts to affect the beam intensity (here IBEAMS) when the position has passed -26 mm. Each point is separated by 1s, since the data acquisition was done at 1 Hz.

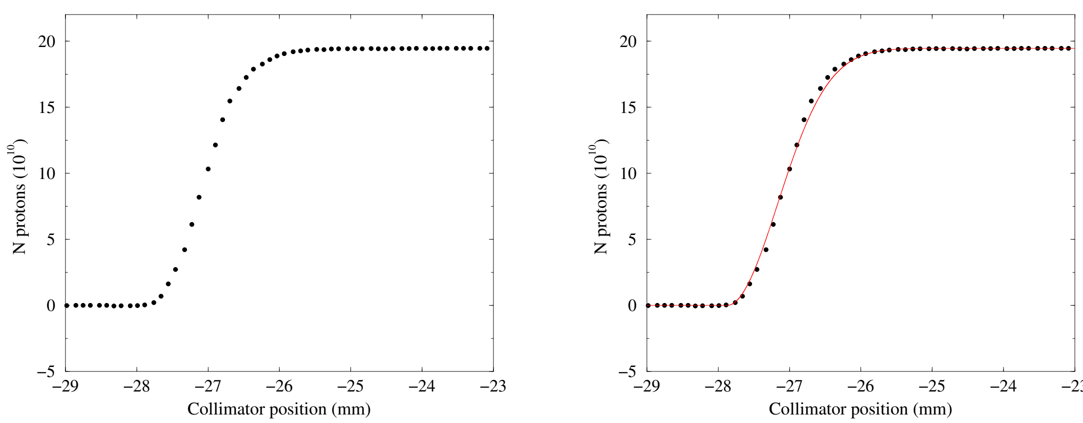

Figure 2: Beam scraping during the 2nd measurement (left), and its fit (right).

The collimator position x_0 where the beam disappears indicates the beam center location, since the particles experience betatron oscillations. With this particular position x_0 and the initial beam intensity before the scraping, the beam size can be determined by fitting the data, assuming a Gaussian beam and using the following expression [6]:

$$N = \begin{cases} N_0(1 - e^{\frac{-(x-x_0)^2}{2\sigma^2}}), & \text{if } x > x_0, \\ 0, & \text{if } x < x_0, \end{cases}$$

where N is the beam intensity, N_0 is the initial value of N, x is the collimator position, and σ is the standard deviation. Fig. 2 (right) shows a fit example for the second measurement. One can notice that the Gaussian approximation seems still to be valid for the second measurement. Using the same method, the beam size for the 1st and 3rd measurement is obtained as shown in Fig. 3. The fit of

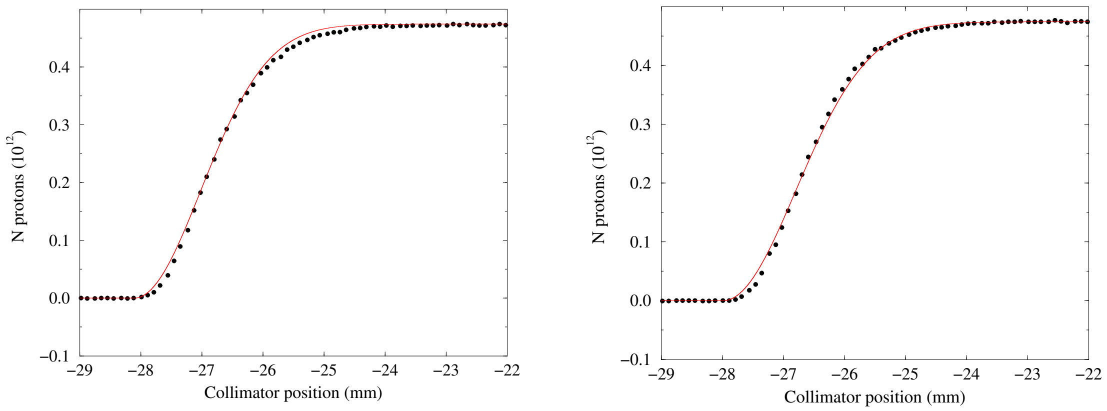

Figure 3: Intensity fits for the two reference measurements,1st(left) and 2nd(right).

the 1st measurement is done with $\sigma = 1.07 \pm 0.02$ mm, the 3rd with $\sigma = 1.19 \pm 0.03$ mm, and the 2nd with $\sigma = 0.70 \pm 0.02$ mm. The 2nd measurement can not be compared with the two references since the scraping mode obeyed different systematics. The emittance can then be obtained as:

$$\varepsilon_N = 6\gamma_L \beta_L \frac{\sigma^2}{\beta_S}$$

from the usual definition of the normalized emittance at FNAL at 95% [7], so that an average for the two reference measurements gives $\varepsilon_N = 15.58 \pm 0.81$ mm.mrad.

3.2 Emittance growth

The emittance growth is estimated by comparing the scraping pattern for the reference measurements with the profile after 1.5 hours as shown in Fig. 4 (left) where the filled symbols are an average of the two reference measurements that are off scale (see Fig. 4 right) since the scraping was not interrupted around 2×10^{11} p. The right plot allows to appreciate the beam displacement between the first and last measurements.

As it has been previously described [3], the evolution of the beam transverse phase-space distribution function f can be described by the Fokker-Planck equation expressed with the action variable I:

$$\frac{\partial f}{\partial t} = D \frac{\partial}{\partial I} \left[I \frac{\partial f}{\partial I} \right]$$

where t is the time, and D is the diffusion coefficient of the beam scattering with residual gas:

$$D = 4\pi\, r_e^2 v_0 \left(\frac{m_e c^2}{p v_0} \right)^2 \sum_i Z_i (Z_i + 1)\, L_c^i \oint\, n_i \beta(s) \frac{ds}{L}$$

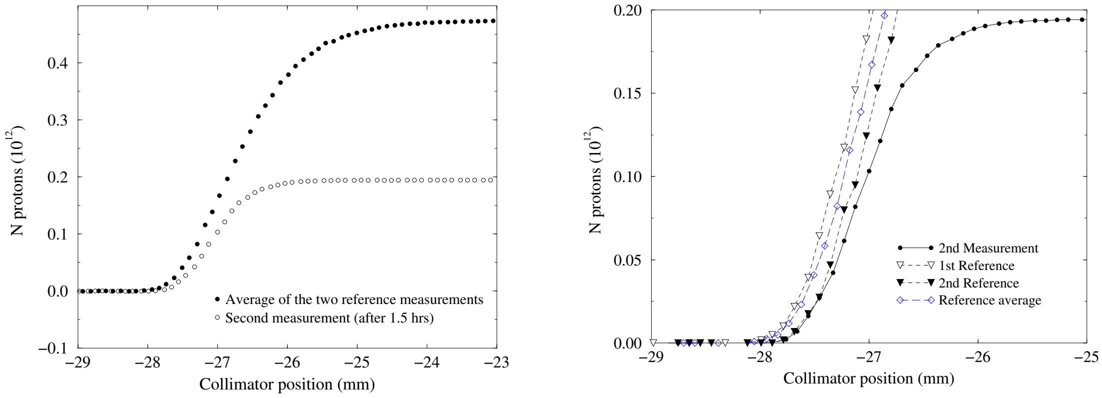

Figure 4: Comparison between reference and delayed scraping profile.

Since the Fokker-Planck equation is not appropriate to handle large changes of the action variable I such as in the case of single scattering where the particle can experience a significant displacement, a formalism correctly describing the diffusion by taking into account both multiple and single coulomb scattering has been developed [3]. The distribution function f obeys:

$$\frac{\partial f}{\partial t} = \int_0^\infty W(I,I')f(I',t)dI'$$

where $W(I,I')$ is related to the probability of the diffusion and includes the coefficient D. The starting distribution f^i has to match the reference measurement and the fact that the beam is scraped before being left for 1.5 hours. Assuming that the initial distribution is Gaussian, the number of protons is:

$$dN(r) = \frac{N_0}{\sigma^2}e^{-\frac{r^2}{2\sigma^2}}rdr$$

where $r^2 = x^2 + (\alpha x + \beta x')^2$. Changing to the action variable $I = \frac{r^2}{\beta}$ [8], then

$$dN(I) = \frac{N_0}{2I_0}e^{-\frac{I}{2I_0}}dI$$

where $I_0 = \frac{\sigma^2}{2\beta}$, so that the initial beam distribution f^i is a truncated decreasing exponential:

$$f^i(I) = \begin{cases} \frac{N_0}{2I_0}e^{-\frac{I}{2I_0}} & \text{if } n < n_{sc}, \\ 0 & \text{if } n > n_{sc}. \end{cases}$$

This initial distribution is then propagated in time by a numerical method. The system is discretized in N bins of the action variable I with an upper boundary value I_b being the admittance of the Tevatron, which at injection was estimated at $I_b = 1.32$ mm.mrad with calculations by A. Drozhdin. The evolution in time of each n value of f is given by:

$$\delta f_n = \frac{\delta t}{\delta I}D\sum_{m=0}^{N-1}\widetilde{W}(n,m)f_m$$

where D is the diffusion coefficient. It is necessary to compute the matrix of $\widetilde{W}_{n,m}$, whose analytical expression is given in [3] and shape is shown on Fig. 6 (right). Each of the elements is related to the probability of the particle to be in the n,m state of action:

$$\begin{pmatrix} \widetilde{W}_{0,0} & \widetilde{W}_{0,1} & \widetilde{W}_{0,2} & \ldots & \widetilde{W}_{0,N} \\ \widetilde{W}_{1,0} & \widetilde{W}_{1,1} & \widetilde{W}_{1,2} & \ldots & \widetilde{W}_{1,N} \\ \vdots & \vdots & \vdots & \vdots & \vdots \\ \widetilde{W}_{N,0} & \widetilde{W}_{N,1} & \widetilde{W}_{N,2} & \ldots & \widetilde{W}_{N,N} \end{pmatrix}$$

The initial distribution referred earlier as f^i is the first line of the array below, which represents the evolution in time of the distribution function $f_I(t)$:

$$\begin{array}{ccccc} f_0(t_0) & f_1(t_0) & f_2(t_0) & \ldots & f_N(t_0) \\ f_0(t_1) & f_1(t_1) & f_2(t_1) & \ldots & f_N(t_1) \\ \vdots & \vdots & \vdots & \vdots & \vdots \\ f_0(t_k) & f_1(t_k) & f_2(t_k) & \ldots & f_N(t_k) \end{array}$$

The time propagation is then given by the δf_n relation. As an example, the transition between $f_0(t_0)$ and $f_0(t_1)$ follows from:

$$f_0(t_1) = f_0(t_0) + \delta f_0(t_0 \rightarrow t_1) \tag{1}$$

where

$$\delta f_0(t_0 \rightarrow t_1) = \frac{\delta t}{\delta I} D(\widetilde{W}_{0,0} f_0(t_0) + \widetilde{W}_{0,1} f_1(t_0) + \widetilde{W}_{0,2} f_2(t_0) + \ldots + \widetilde{W}_{0,N} f_N(t_0)) \tag{2}$$

and the same apply for all the elements of the f distribution.The δf_n relation implies a convergence condition on the time step δt, i.e. $\delta t < \delta I^2$. The simulation then runs over k iterations of a dimensionless time step $\bar{\delta t}$ satisfying this condition and for a specific k, the quantity $\int f(I,t)dI$ is calculated and gives a profile similar to a beam intensity scraping pattern. The iteration stops when the obtained profile matches the experimental data. Fig. 5 (left) shows the distribution function $f(I)$ in action and its evolution trough time, with the initial truncated exponential at the start of the simulation. Fig. 5 (right) shows the corresponding number of protons, i.e. $N = \int f(I,t)dI$.

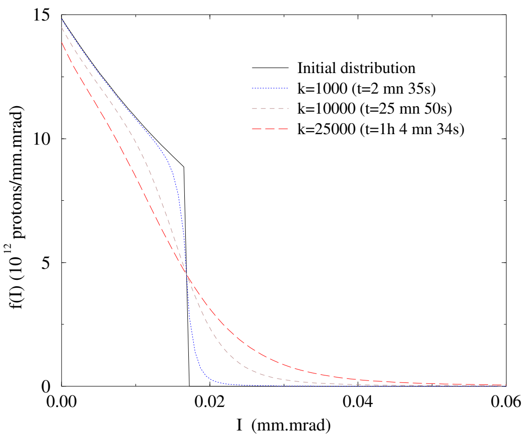

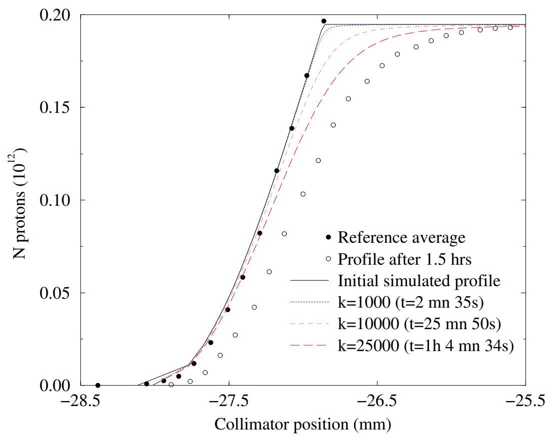

Figure 5: $f(I)$ (left) and corresponding number of particles without beam position correction (right).

Matching the initial distribution f^i as shown in Fig. 5 (right) is strongly dependent on the bin size of the action variable; the finer the bin in action δI is, the closer is the initial value of $N = \int f(I,t)dI$ to

the starting intensity, although a too small δI leads to huge matrix sizes and computing time due to the convergence requirement. With an adequate δI, the index n_{sc} introduced earlier that represents the scraping, is obtained when $\int f(I,t)dI$ equals the starting intensity i.e. the intensity value at the moment the vertical collimator has stopped its course toward the beam and is being retracted. There was a period of 68 s where the beam was still scraped even though the collimator was not moving, probably due to a beam displacement, making the starting intensity at 1.95×10^{11} p. The evolution in action of the distribution function is illustrated in Fig. 6 (left) where it is shown how a particle with a specific action will easily be displaced on a short range (the two positive peaks - multiple Coulomb scattering) and possibly on a long range (slope of these two peaks - single Coulomb scattering), but will be displaced from its current location (negative peak).
With a dimensionless step in time set to $\bar{\delta t} = 2.5 \times 10^{-7}$, chosen in concordance with the convergence requirement, the data are best fit for $k = 36000 \pm 100$ as shown in Fig. 6 (right), with a correction on the beam position as this can not be anticipated by the model.

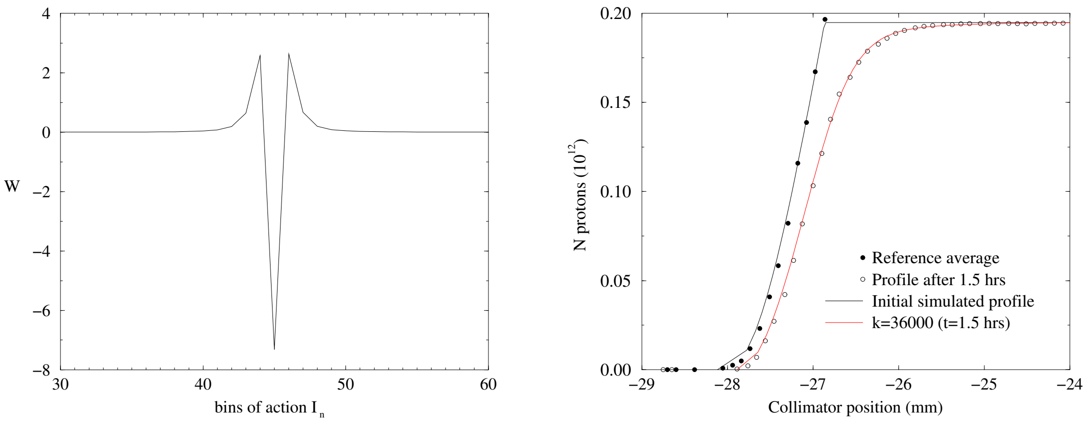

Figure 6: Function $\widetilde{W}$ responsible for change in action (left) and best match to the data of the 2nd measurement (right).

For these calculations, the diffusion coefficient was set to $D = 1$, as a dimensionless quantity. It is then possible to extract its real value:

$$D\,\bar{\delta t} = 2.5 \times\ 10^{-7}$$

with a good agreement obtained for $k = 36000 \pm 100$, hence for $k\ \delta t = 5427$ s (1.5 hrs)

$$\delta t = \frac{5427}{k} = 0.150 \pm 0.004 s.$$

This gives:

$$D = \frac{2.5 \times\ 10^{-7}}{\delta t} = 1.66 \pm 0.05 \times\ 10^{-6} mm.mrad/s$$

i.e. a corresponding diffusion coefficient of the beam of $5.97 \pm 0.18 \times 10^{-3}$ mm.mrad/h on average. This can be expressed in terms of the emittance growth with the following relation:

$$\frac{d\varepsilon_n}{dt} = 3\gamma_L\beta_L D,$$

i.e. the emittance growth of about 2.86 ± 0.09 mm.mrad/h (normalized at 95%).

3.3 Lifetime and residual gas composition

The intensity drop of the beam during the 1.5 hours was parametrized with a second order polynomial expression which leads to a lifetime of the beam varying between 1040 and 970 hours. With an average beam lifetime around 1000 hours and the value of the beam emittance growth found in (3.2), some partial pressure of residual gases in the beam pipe can be estimated.

Fig. 7 (left) shows the different pressures of gas species and how they relate to the ratio of the emittance growth found experimentally $EG_{exp} = 2.86\pi$ mm.mrad/h, with a calculated one, EG_{cal}. Each of these EG_{cal} - noted $\dot{\varepsilon}$ - curves were obtained with the following relation:

$$\dot{\varepsilon}(\beta_S, P, Z_i, k_i, \gamma_L) = 6\frac{\beta_S}{2}2.46\ P\ (\frac{13.6}{938})^2\ \frac{1}{\gamma_L}\ 8.63469\ 10^6\ 3600\sum_i k_i\ Z_i\ (Z_i + 1)$$

where β_S is the average β-function in the Tevatron ($\sim$70 m), P is the pressure, Z_i is the atomic number of the i element with k_i atoms per molecule, 8.63469 is the Coulomb logarithm taken constant consistently with the treatment in (3.2), and γ_L is the Lorentz factor. The lower curve corresponds to Ar, then CO_2, CO and N_2, C_2H_2, CH_4, He and the upper curve is H_2. It reads as the expansion of the beam with the coefficient EG_{exp} is obtained with a pressure of 3.38×10^{-8} Torr of H_2, if molecular hydrogen would be the only residual gas. It can be seen that as expected from the Z^2 dependence of the emittance growth, a lower pressure of a heavy gas leads to the same diffusion than a much higher pressure of a lighter gas.

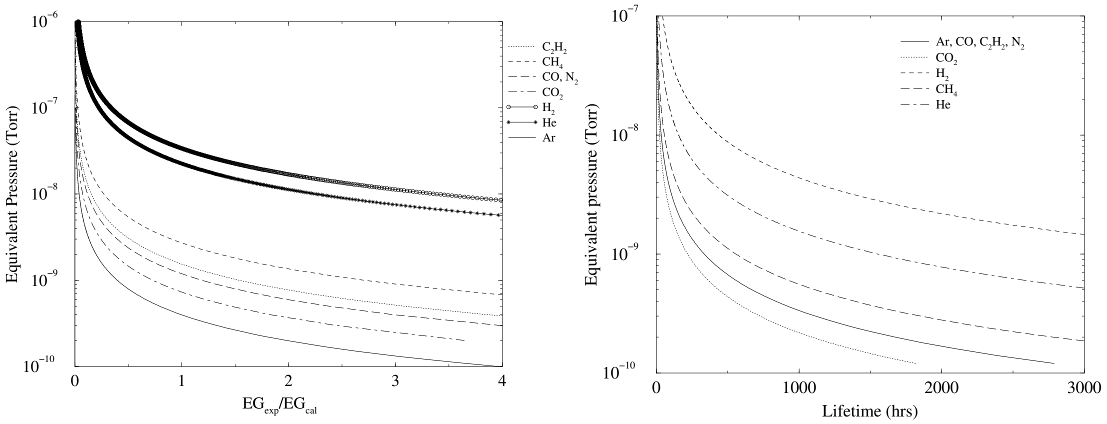

Figure 7: Evolution of the partial gas pressure with emittance growth (left) and with lifetime (right).

Fig. 7 (right) shows the influence of the partial pressure on the lifetime. H_2 is the upper curve, then He and CH_4. Ar,CO, C_2H_2, N_2 are hardly distinguishable and grouped in one curve, and finally CO_2 is the lowest. Lifetimes were obtained with the relation:

$$\tau(k_i, A_i, P) = \frac{1}{3600\ 3\times 10^{10}\ \frac{\mathcal{N}}{22400}\ \frac{P}{760}\ 389\times 10^{-27}\ \sum_i k_i (\frac{A_i}{14})^{\frac{2}{3}}}$$

where $\mathcal{N}$ is the Avogadro number, P is the pressure, A_i is the atomic mass of the i element with k_i atoms per molecule, using a A_i-scaling with the cross section on nitrogen at 150 GeV (around 389 mb as calculated by S. Striganov), except for H_2, where the microscopic cross section is taken equal to 30 mb, assuming that this is the total cross section that is responsible for the lost of particles. This is an approximation, while the inelastic part of the cross section (285 mb) should lead to protons removal, only a part of the elastic cross section (104 mb) will give deflection angles such that the protons will be lost. As given in [9], Table 1 resumes for each gas, the particular pressure value that leads to a ratio $\frac{EG_{exp}}{EG_{cal}} = 1$, and the pressure that leads to the lifetime found experimentally (1000 hours). It can be seen that due to the variation in $\frac{1}{A^{\frac{2}{3}}}$ for the lifetime , the equivalent pressure for Ar (40 amu) is similar to the one of N_2 (28 amu) or CO (28 amu).

Gas species	H_2	N_2	Ar	C_2H_2	CH_4	CO	CO_2	He
P (nTorr) ($\dot{\varepsilon}$)	33.8	1.2	0.4	2.7	2.7	1.2	0.7	22.5
P (nTorr) ($Lifetime$)	4.35	0.34	0.34	0.34	0.56	0.34	0.22	1.55

Table 1: Equivalent partial pressure for the experimental emittance growth and lifetime

with an uncertainty of these values of about 3%. There are discrepancies between the equivalent pressure calculated from the lifetime and from the emittance growth, as the assumption of 100% of a particular specie for the residual gas is naturally not accurate and only has an indicative function. However, it seems that the gas composition of the Tevatron has on overall impact on the beam similar to a condition where Ar would be the only gas present in the beam pipe. By calculating the product $\dot{\varepsilon}\tau$ using both experimental values found for the emittance growth and the lifetime, it is possible to obtain the following quantity:

$$\mathcal{R} = \frac{\sum_i k_i \; Z_i \; (Z_i + 1)}{\sum_i k_i A_i^{\frac{2}{3}}} = 34.66 \pm 2.47$$

It is then interesting to compute the same quantity for each gas:

Gas	H_2	N_2	Ar	C_2H_2	CH_4	CO	CO_2	He
$\mathcal{R}$	2	9.64	29.26	7.04	5.40	9.83	10.37	2.38

It was also attempted to solve both equations for the emittance growth and the lifetime, with a set of gases and partial pressures satisfying both experimental values. A trial based on gas proportions from a June 2002 RGA scan at B4 (77°K) failed to satisfy both equations, which is not surprising since it is likely that gas composition and pressure vary along the accelerator. An interesting point to note though, is out of four noticeable peaks on this RGA scan, one of them is at $A = 40$, which seems to indicate the presence of Argon at the location of the scan.

4 Conclusions

An experiment using the Tevatron beam at 150 GeV with protons only was set up with the aim of investigating beam emittance growth, lifetime and residual gas present in the beam pipe. It was verified that the beam shape was close to a Gaussian with value of emittance and lifetime consistent with other measurements. It was shown that the formalism of transverse expansion due to residual gas is able to reasonably explain the beam behavior despite the absence of nuclear modeling for the beam's diffusion in unidimensional treatment, and provided a value for the emittance growth within the range of the expectations. This, combined with the beam lifetime of 1000 hours, seems to suggest an overall averaged gas composition with properties close to the Argon gas with the pressure $\sim 3-4 \times 10^{-10}$ Torr. One year earlier, [10] discussed an average pressure of 1.6×10^{-9} Torr, although this value was obtained based on N_2 gas with a different method.

5 Acknowledgments

We are grateful to A. Burov, A. Drozhdin, A. Jansson, N. Mokhov, R. Moore, S. Nagaitsev, V. Shiltsev, D. Still, S. Striganov, and M. Syphers for useful discussions.

References

[1] N. V. Mokhov, V. I. Babelkov, “Beam and Luminosity Lifetime”, Handbook of Accelerator Physics and Engineering, Ed. by A.W.Chao and M.Tigner, p.218, World Scientific (2002).

[2] D. Allen, Private discussion, from June,13th 2002 RGA scans of the B4 section, at cold and liquid nitrogen temperature.

[3] V. A. Lebedev, S. Nagaitsev, “Particle Diffusion due to Coulomb Scattering”, Fermilab-CONF-02/099-T(2002).

[4] A. I. Drozhdin et al, “Beam Loss and Backgrounds in the CDF and DØ Detectors due to Nuclear Elastic Beam-Gas Scattering”, Fermilab-FN-734 (2003).

[5] A. I. Drozhdin, Private discussion.

[6] A. Jansson et al, “Collimator Scans to Measure Tevatron Emittance”, Fermilab-Beams-doc-393-v2 (2003).

[7] D. A. Edwards, M. J. Syphers, An Introduction to the Physics of High Energy Accelerators, Wiley, N.Y.(1993).

[8] M. J. Syphers, “Beam-Gas Scattering Lifetimes in the Fermilab Main Ring”, Fermilab-FN-484 (1988).

[9] V. A. Lebedev et al., Report on Tevatron Modeling and Accelerator Physics, FNAL report for the summer 2003 DOE review, FNAL, June 2003.

[10] R. Moore, V. Shiltsev, “Estimate of the Tevatron vacuum on the basis of the known pressure rise at F11”, Fermilab-Beams-doc-240 (May/June 2002).